Meteoritics & Planetary Science 39, Nr 6, 821–829 (2004)
Abstract available online at http://meteoritics.org

Magnetostratigraphy of the impact breccias and post-impact carbonates from borehole Yaxcopoil-1, Chicxulub impact crater, Yucatán, Mexico

Mario REBOLLEDO-VIEYRA[1, 2*] and Jaime URRUTIA-FUCUGAUCHI[2]

[1]Laboratoire des Sciences du Climat et l'Environnement, Unité de Recherche Mixte CNRS-CEA, Gif-sur-Yvette, France
[2]Laboratorio de Paleomagnetismo, Instituto de Geofisica, UNAM, Coyoacán, Mexico City, Mexico
*Corresponding author. E-mail: marior@lsce.cnrs-gif.fr

(Received 29 August 2003; revision accepted 1 March 2004)

Abstract–We report the magnetostratigraphy of the sedimentary sequence between the impact breccias and the post-impact carbonate sequence conducted on samples recovered by Yaxcopoil-1 (Yax-1). Samples of impact breccias show reverse polarities that span up to ~56 cm into the post-impact carbonate lithologies. We correlate these breccias to those of PEMEX boreholes Yucatán-6 and Chicxulub-1, from which we tied our magnetostratigraphy to the radiometric age from a melt sample from the Yucatán-6 borehole. Thin section analyses of the carbonate samples showed a significant amount of dark minerals and glass shards that we identified as the magnetic carriers; therefore, we propose that the mechanism of magnetic acquisition within the carbonate rocks for the interval studied is detrital remanent magnetism (DRM). With these samples, we constructed the scale of geomagnetic polarities where we find two polarities within the sequence, a reverse polarity event within the impact breccias and the base of the post-impact carbonate sequence (up to 794.07 m), and a normal polarity event in the last ~20 cm of the interval studied. The polarities recorded in the sequence analyzed are interpreted to span from chron 29r to 29n, and we propose that the reverse polarity event lies within the 29r chron. The magnetostratigraphy of the sequence studied shows that the horizon at 794.11 m deep, interpreted as the K/T boundary, lies within the geomagnetic chron 29r, which contains the K/T boundary.

INTRODUCTION

After a successful UNAM Scientific Drilling Program in the Chicxulub impact crater conducted in the late 1990s (Rebolledo-Vieyra et al. 2000; Urrutia-Fucugauchi et al. 1996), where a sequence of impact breccia from the Chicxulub impact crater was recovered for the first time (Fig. 1), the International Continental Scientific Drilling Program (ICDP) in collaboration with UNAM, along with other organizations such as GFZ, Germany, DOSSEC, USA, and the PITSA drilling company, Mexico, developed a drilling project for an additional borehole with continuous core recovery at a site located in the southern sector of the crater.

The objectives of this new drilling project within the crater are to recover impact-generated lithologies and, possibly, underlying target rocks, to investigate effects of the impact on the target rocks, to evaluate scenarios concerning global effects on live-supporting systems, and to conduct research on the impact cratering process.

Before the drilling of the ICDP Yaxcopoil-1 (Yax-1) borehole, several geophysical surveys were conducted in the area, such as seismic reflection (Bell et al. 2004; Snyder and Hobbs 1999; Brittan et al. 1999; Morgan and Warner 1999; Christeson et al. 1999), aeromagnetism (Pilkington et al. 2000; Ortíz-Alemán 1999), gravimetry (Sharpton et al. 1992; Hildebrand et al. 1991), and several other surveys (Campos-Enriquez 1997; Pope et al. 1996). With these data available, during a workshop sponsored by ICDP in the city of Mérida in 1998, a group of 14 scientists discussed drilling a deep scientific borehole within the crater limits (Urrutia-Fucugauchi et al. 2001). After the analyses of geophysical data and the evaluation of site availability and logistical details, eventually, a drilling site located some 60 km southwest from the crater center was selected. Yax-1 was drilled between December 2001 and March 2002 and reached a depth of 1511 m from ground level. Here, we report the results of a detailed magnetostratigraphy study (2–5 cm interval sampling) of a critical interval that includes the contact between the impact breccias (794.66 m) and Tertiary carbonates (793.83 to 794.11 m) (Fig. 2a).

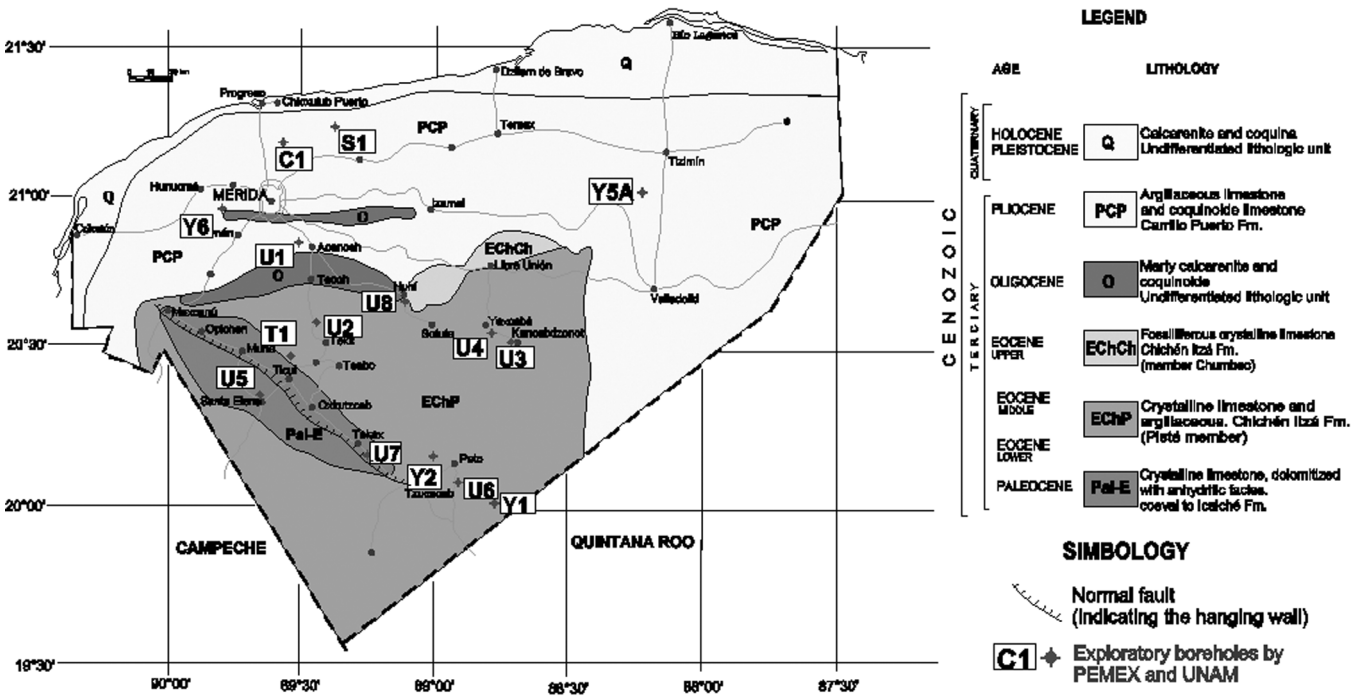

Fig. 1. Location map showing the boreholes from the UNAM's Chicxulub Scientific Shallow Drilling program (U1 = UNAM-1; U2 = UNAM-2; U3 = UNAM-3; U4 = UNAM-4; U5 = UNAM-5, U6 = UNAM-6; U7 = UNAM-7, and U8 = UNAM-8) that recovered impact breccias; PEMEX boreholes Y-1 = Yucatán-1; Y5a = Yucatán-5a; C-1 = Chicxulub-1; S-1 = Sacapuc-1; and T-1 = Ticul-1. Yax-1 is from the Chicxulub Scientific Deep Drilling Program. Modified from Rebolledo et al. (2000).

AGE CONSTRAINTS

Several $^{40}Ar/^{39}Ar$ ages for melt samples from the Chicxulub-1 (Fig. 2b) borehole are available, all of which yielded ages of 64.98 ± 0.05 Ma (Swisher et al. 1992) and 65.2 ± 0.4 Ma (Sharpton et al. 1992). As for previous paleomagnetic studies in Chicxulub impact breccias, Urrutia-Fucugauchi et al. (1994) reported a reversed magnetic polarity for the same sample from borehole Yucatán-6 (Fig. 2b) and associated it to chron 29r, which bears the K/T boundary, based on the radiometric dates reported by Swisher et al. (1992) and Sharpton et al. (1992).

LITHOLOGY

Yax-1 is located 40 km southwest of Mérida, Mexico and approximately 60 km from the center of the Chicxulub structure (Fig. 1). Yax-1 recovered a continuous sequence from 400 m to 1511 m below the surface (Fig. 2a and 2b). The contact between the impact breccias and the carbonate sequence was found at 794.63 m (from ground level). The 100 m-thick impact breccia overlies a 616 m-thick sequence of very fine to fine-grained limestone, dolomite, and anhydrite with some dikes of impact breccia and impact melt (Fig. 4a). The impact breccia (suevite) consists primarily of clasts from these underlying shallow-water lithologies, some crystalline rocks of continental basement origin, and devitrified glass fragments and spherules (Stinnesbeck et al. 2003). The upper 15 m of the impact unit is composed of reworked breccia that is stratified with alternating layers of upward fining clasts (3–5 cm at the base to 2–5 mm at the top), coarse cross-bedding structures, and gray friable sand layers in the top meter, all of which indicate reworking and current transport after deposition of the impact breccia. Above these reworked breccia layers are finely laminated dolomitic limestone and limestone layers.

Keller et al. (2003) reported a 49–50 cm-thick layer of laminated dolomitic limestone with some small-scale (2 cm) cross-bedding and flaser bedding between the top of the impact breccia and the K/T boundary. According to Keller et al. (2003), the entire interval is rich in late Maastrichtian planktic foraminifera, though preservation is variable depending on the degree of dolomitization.

The dolomitic calcareous unit above the redeposited suevitic breccia contains few reworked planktic foraminifera, for which Arz et al. (2004) report a different age range for the planktonic foraminifera—from Albanian to Maastrictian—and which is interpreted as the uppermost portion of the sedimentary infill of the crater.

The K/T boundary in Yax-1 is represented by a thin, laminated, dark marly clay layer likely of redeposited impact material located at ~794.11 m, about 50 cm above the impact breccia. The boundary is characterized by a 2–3 cm-thick dark gray-green marly limestone with a 3–4 mm-thick green glauconitic clay (Keller et al. 2004).

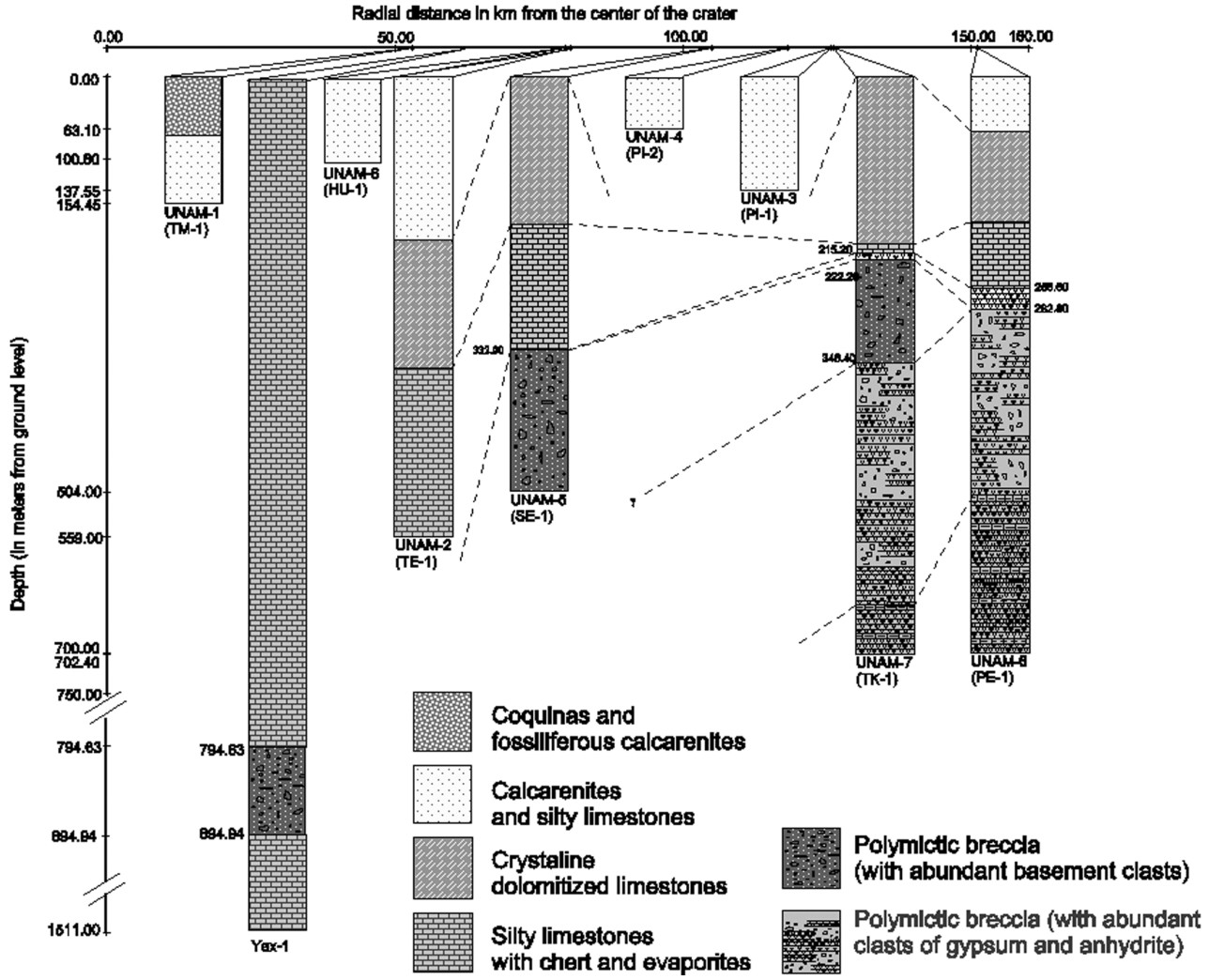

Fig. 2a. Lithologic columns from the Chicxulub Scientific Shallow Drilling Program, including the lithologic column of Yax-1. Modified from Rebolledo et al. (2000).

PALEOMAGNETIC ANALYSES

Discrete specimens from the Yax-1 core were collected from the working half of the cores deposited in the Chicxulub Scientific Drilling Project (CSDP) Core Repository of the Instituto de Geofisica, UNAM, in Mexico City. Yax-1 specimens are 2.5 cm^3 cubes (if the conditions of the samples allowed it) that were analyzed in a 2G DC-SQUID cryogenic magnetometer with a background noise of 1×10^{-8} A/m in a magnetically shielded room at the laboratory of paleomagnetism of the Laboratoire des Science du Climat et de l'Environnement, Gif-sur-Yvette, France. Samples were demagnetized using two consecutive methods, alternating field (AF) from 0 to 100 mT, with 20 mT steps to identify and eliminate a possible secondary magnetization. After the AF process, samples were thermally demagnetized from 100 °C to 650 °C in 25 °C steps. Measurement of the low-field magnetic susceptibility was done in a Minikappa susceptibility meter, from Geofysika, for each sample before any demagnetization process and after every thermal step to survey any modification of the magnetic minerals due to oxidation.

RESULTS

Yax-1 specimens were used to construct the magnetostratigraphy of the contact between the breccias and the carbonates. Data were plotted in standard orthogonal diagrams (Zijderveld vector plots), and the characteristic direction of the magnetic signal was estimated using the least-squares method of Kirschvink (1980) (Fig. 3). Since the samples came from a continuous core with no declination measured on site, only the calculated magnetic inclination was used to construct the magnetostratigraphy; however, declination was kept to assess the stability of the magnetic signal during the demagnetization process.

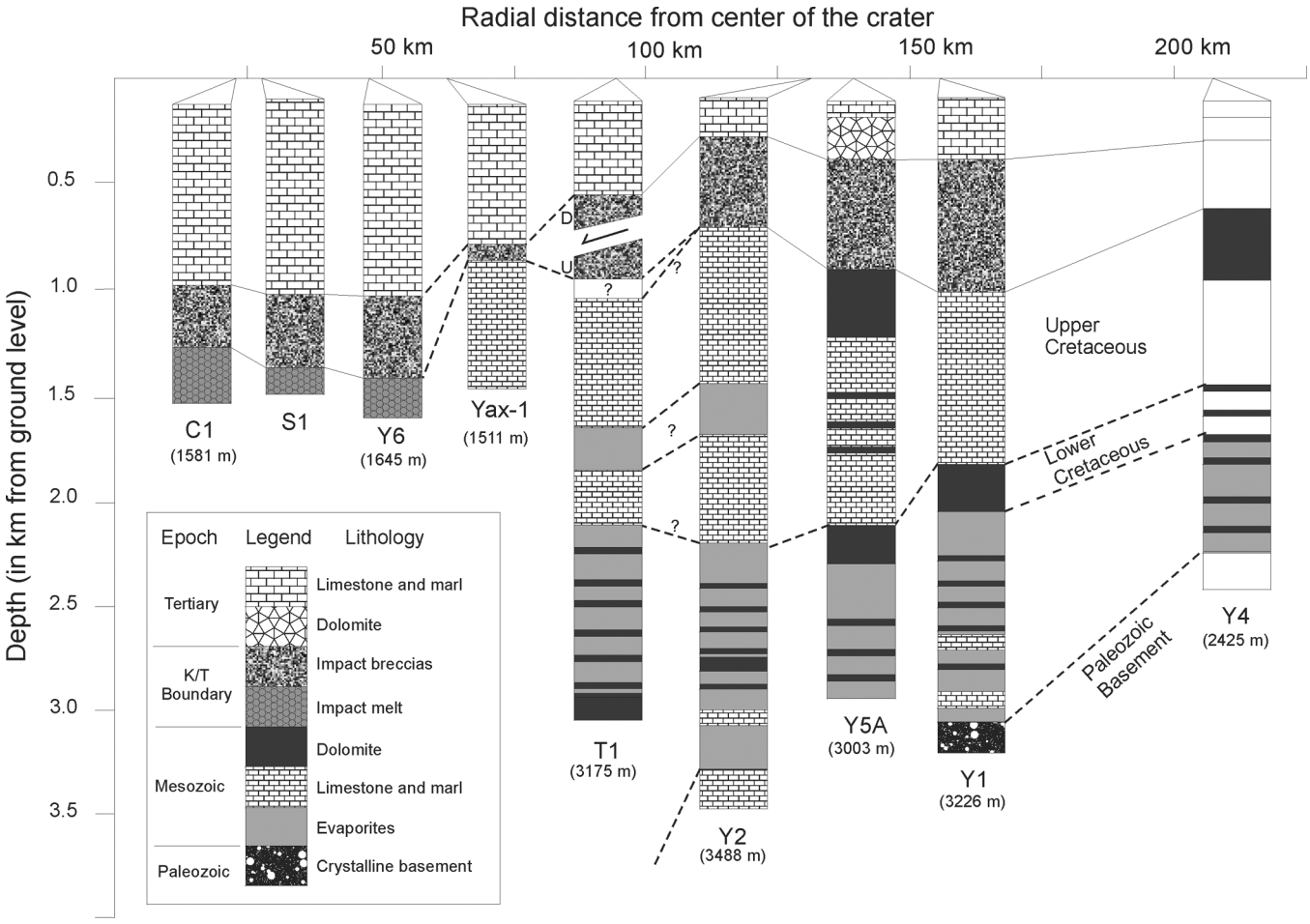

Fig. 2b. Lithologic columns from the exploratory boreholes from PEMEX, including the lithologic column of Yax-1. Modified from Ward et al. (1995).

NRM AND KÖNIGSBERGER RATIO

We present the paleomagnetic parameters for each sample in Table 1. The natural remanent magnetism (NRM) is not very strong (exceptions are samples Yax-1_794.14 and Yax-1_794.35; Table 1) and supports our hypothesis that the detrital remanent magnetism (DRM) is the main mechanism for acquiring magnetization. Analyses of thin sections from the carbonate sequence studied showed that there is an important component of dark minerals and glass; the concentration of this material decreases upward, with the highest concentration close to the contact with the impact breccias.

As for the Königsberger ratio (Q), it lies within the expected range for sedimentary rocks (Q ≤1) for most of the samples. The exceptions are Yax-1_793.87, Yax-1_793.99, Yax-1_794.27, and Yax-1_794.35, which are higher and lay in the range for volcanic rocks (Q = 1–10). We should mention sample Yax-1_794.14 separately since its Q is higher than 14, which is within the range of fast quenching volcanic rocks. We consider that these exceptions are related to the high contents of impact material within the samples. These samples correspond to intervals with clear interlayering of impact material (Fig. 4). These layers vary in thickness from few mm to 1 cm. Sample Yax-1_794.14 is only 3 cm below the postulated K/T limit in Yax-1, which is represented by a ~2 cm-thick layer of a microconglomerate rich in glauconite (Keller et al. 2003) and impact material; we associate this highly magnetic character of the samples to the enriched impact material.

MAGNETOSTRATIGRAPHY

We developed a magnetostratigraphic sequence constructed with 17 samples that span 79 cm (793.87 m to 794.66 m) of the sequence that includes the contact between the impact breccias and the first part of the carbonate sequence recovered by Yax-1 (Fig. 4). The sampled interval includes what some authors, based in micropaleontological criteria, consider to be the Cretaceous-Tertiary (K/T) boundary at 794.11 m (e.g., Keller et al. 2003; Smit et al. 2003). In the analyses, we also include some samples taken

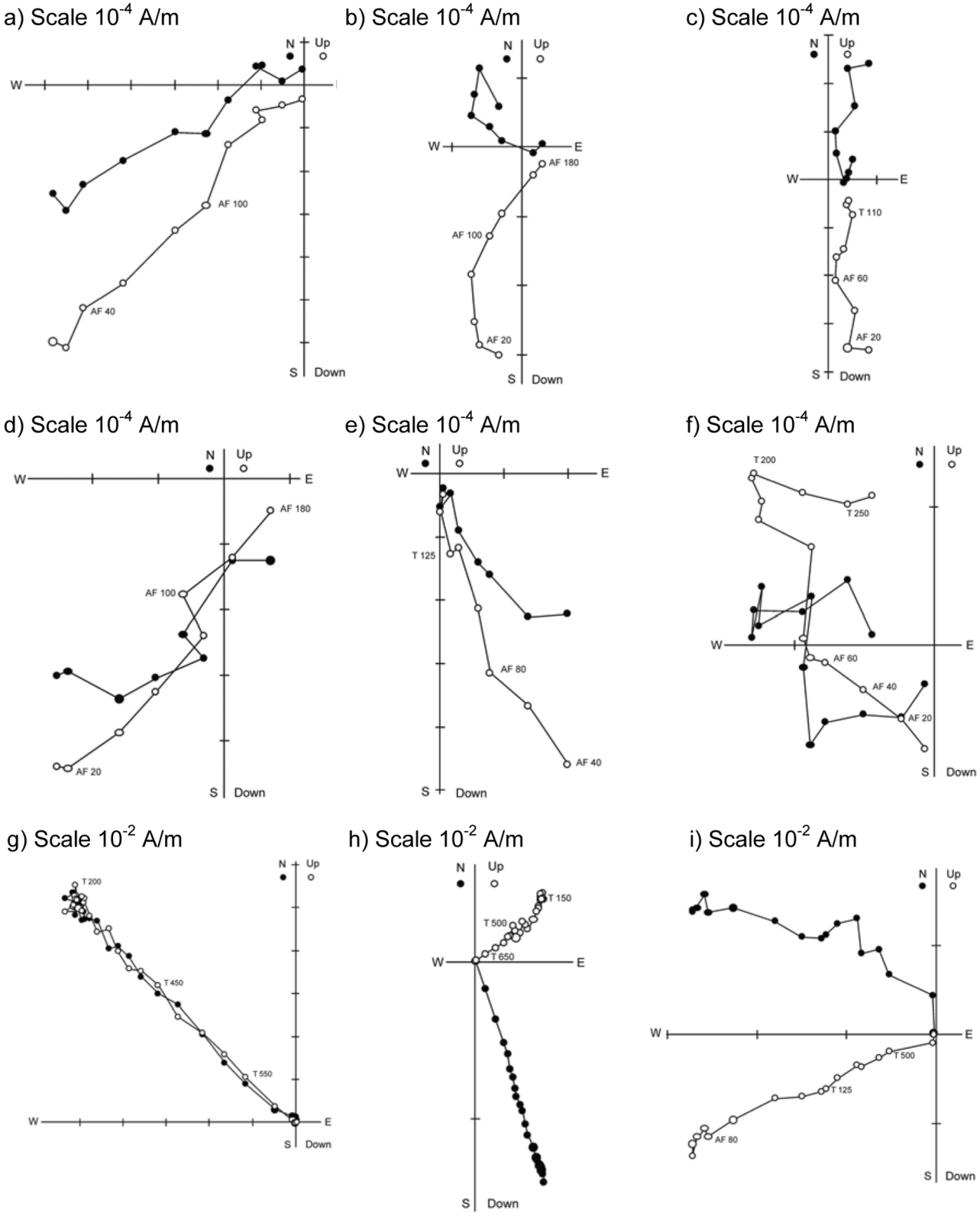

Fig. 3. Orthogonal diagrams of the trajectories from alternating field (units in mT) and thermal demagnetization (units in °C) processes of samples used in the magnetostratigraphy: a) Yax-1_793.87; b) Yax-1_793.92; c) Yax-1_793.99; d) Yax-1_794.02; e) Yax-1_794.04; f) Yax-1_794.12; g) Yax-1_853.88; h) Yax-1_876.20; i) Yax-1_879.63. See Table 1 for the calculated paleomagnetic parameters.

Table 1. Paleomagnetic parameters calculated for the samples analyzed in this study.[a]

Sample no.	Depth	NRM	κ	Dec	Inc	MAD	Q	N	Lithology
Yax-1_793.87	793.87	872	11	245.5	44.3	2.2	2.26	6	Laminated dolomitic limestone
Yax-1_793.92	793.92	314	8	302.2	53.6	4.3	1.1	4	
Yax-1_793.99	793.99	437.2	4	13.4	58.6	5.4	3.12	4	
Yax-1_794.02	794.02	590.1	30	191.4	45.0	6.9	0.56	4	
Yax-1_794.04	794.04	547.8	27	152.3	54.0	3.9	0.58	5	
Yax-1_794.08	794.08	388.9	20	351.1	–18.9	6.6	0.55	4	
Yax-1_794.12	794.12	78.5	20	280.9	–40.1	6.1	1.12	3	Fine laminate dolomitic limestone with cross-bedding structures; interbedded greenish fine sand layers
Yax-1_794.14	794.14	81329.2	155	359.8	–5.1	4.7	14.99	6	
Yax-1_794.16	794.16	185.8	43	307.2	–76.8	4.3	0.12	4	
Yax-1_794.20	794.20	191.0	0	275.2	–47.4	5.3	–	5	
Yax-1_794.21	794.21	134.3	0	266.1	–41.4	2.5	–	3	
Yax-1_794.27	794.27	826.8	29	141.9	–12.5	3.0	1.57	3	
Yax-1_794.35	794.35	1169.9	15	180	–23.6	10.8	2.7	4	
Yax-1_794.38	794.38	61.6	9	183.4	–41.8	8.8	0.2	4	
Yax-1_794.44	794.44	24.3	38	223.7	–54.1	7.8	0.018	3	
Yax-1_794.59	794.59	91.8	8	231.1	–11.7	5.7	0.32	4	
Yax-1_794.66	794.66	45.0	0	83.7	–12.6	8.5	–	3	Redeposited suevite, melt-rich, clast-size sorted, fine-grained
Yax-1_853.88	853.88	896489.5	4820	315.0	–35.9	0.9	5.166	5	
Yax-1_876.20	876.20	151763.5	2130	162.5	–14.3	2.2	1.98	28	
Yax-1_879.63	879.63	32326.1	1890	323.7	10.6	3.8	0.475	8	

[a]Sample no. = Code sample as registered in the CSDP database; Depth = depth in m from ground level; NRM = natural remanent magnetism, × 10^{-6} A/m; κ = magnetic susceptibility, dimensionless, × 10^{-6} S.I.; Dec = declination (degrees); Inc = inclination (degrees); MAD = maximum angular deviation (degrees); Q = Könisgberger ratio (Q = NRM/κHe), where κ = magnetic susceptibility and He (Earth's magnetic field) = 35 A/m; N = number of demagnetization steps used for the least-square fit.

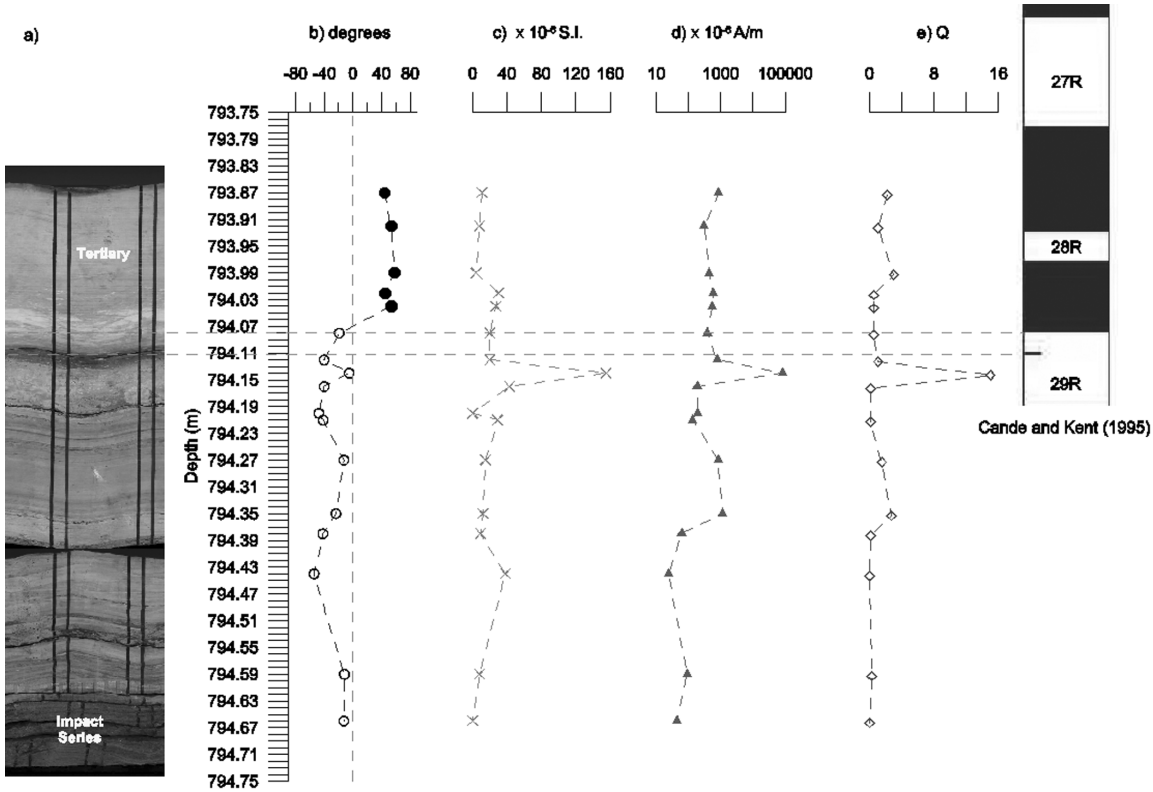

Fig. 4. Magnetostratigraphy of upper impact breccias and the lower Tertiary carbonate section: a) lithological digital image of section; b) inclination; c) low-field susceptibility; d) natural remanent magnetism; e) Königsberger ratio (NRM/κHe). The lower dashed line indicates the position of the K/T boundary as proposed by Smit et al. (2004) and Keller et al. (2003). The upper dashed line indicates the stratigraphic position of polarity change from magnetochron 29r to 29n. The solid line indicates the top of magnetochron 29n.

from some of the impact breccia units described as not redeposited by Dressler et al. (2003) to compare the magnetic signal with the top breccias that are interpreted as redeposited; however, we did not include those samples to construct the magnetostratigraphy.

A first interesting result is the behavior of the low-field magnetic susceptibility along the sequence, which in the samples from the Tertiary dolomites is within the diamagnetic range (0×20^{-6} S.I.); however, some of the carbonate samples show values above this range ($10–30 \times 10^{-6}$ S.I.). We consider that the small amount of ferrimagnetic particles from the reworked impact material, embedded in the carbonate matrix, could be the source of this magnetic susceptibility, and it increases to values up to 155×10^{-6} S.I. (Table 1).

During drilling operations, care was taken to have non-magnetic drilling bits along the whole coring to avoid remagnetization of the cores; however, to be absolutely sure that the samples did not acquire a secondary remagnetization, we performed the first dema0gnetization analyses with AF. Samples from the breccia, which exhibit normal polarity, did not show any evident secondary remagnetization (Fig. 3); on the other hand, samples from the sedimentary sequences between 794.63 and 794.08 m present reverse polarity and a rather unstable demagnetization path (Fig. 3). This suggests that we needed to be extremely careful with the calculation of the mean direction of the demagnetization path and the resulting polarity. All the samples above 794.11 m had a normal polarity, a weak secondary remagnetization that was removed after the 60 mT AF demagnetization treatment, and exhibited a stable demagnetization path.

In Fig. 4b, we show the constructed magnetostratigraphy, starting from the last sample recovered from the impact breccias up to the first 24 cm above from the proposed K/T boundary (794.11 m) (Keller et al. 2003; Arz et al. 2004; Smit et al. 2004). The first 12 samples, from the bottom upward, show reverse polarity, where the first sample considered belongs to the re-worked impact breccia. These breccias are considered to be equivalent to impact breccias recovered in other boreholes (Y-6, C-1, UNAM-5, UNAM-7) and are assumed to have the same age.

In the last 17 cm of the sequence studied, we collected four samples from laminated dolomites that yielded rather stable demagnetizing paths with normal polarity (Fig. 3). Keller et al. (2003) report a ~100 Kyr hiatus at the K/T boundary, as the earliest Danian fossil zone (P0) is absent. The change in polarity between 794.04 m and 704.08 m deep (from ground level) most likely represents the change from 29r to 29n (64.745 Myr; Berggren et al. 1995). However, until more measurements are made up-section, we cannot be sure that it does not represent the short normal polarity event reported in Lerbekmo et al. (1996).

DISCUSSION

Our working hypothesis is that the reverse polarity event, which includes the impact breccias and the first 56 cm of the carbonate sequence on top of the breccias, corresponds to chron 29r; the reverse polarity continues up to a depth of 794.07 m and includes the horizon defined as the K/T boundary (794.11 m). There is a lack of samples in the interval between 794.59 m and 794.44 m because the demagnetization trajectories of the samples collected in this interval did not show a lineal and stable behavior; therefore, we discarded them. We interpret this behavior either as a consequence of the cross-bedded, large grain-size layers interstratified in the sequence or as the absence of any magnetic minerals. Even though the rest of the sequence is similar (i.e., laminar dolomites with thin slightly larger grain size, interstratified horizons), we were able to obtain a polarity for the rest of the samples. However, we acknowledge that the Fisher statistics calculated for the samples from the carbonate section are very unstable and not completely reliable and should be taken with some reservation. We interpret this material as reworked impact material from slumping and as being the magnetic carrier, which, in turn, will support the hypothesis that DRM is the main mechanism for acquiring magnetization. No clear evidence of chemical or hydrothermal alteration could be identified in the analyzed thin sections.

Considering that we observe the change of polarity from 29r to 29n at between 794.04 and 794.08 m, the sedimentary sequence between the K/T boundary and the reversal is 3–7 cm thick. This suggests that a considerable portion of the sequence of the base of Paleocene is missing. At this time, we have not dated any of the Yax-1 samples to be able to correlate the normal polarity as 29n. We base our interpretation on the presence of the Danian planktic foraminifera that indicate the upper zone of P1c (e.g., absence of *P. eugubina* and presence of *premurica inconstans, E. trivialis,* and *globanomalina pentagona*) (Keller et al. 2004). The magnetostratigraphic data cannot be used to estimate how much of the basal Paleocene is missing and likely marks a hiatus that Arz et al. (2004) indicate as spanning the *G. cretacea, Pv. eugubina,* and part of the *P. pseudobulloides* biozones.

CONCLUSION

The top two units of the impact breccias have been redeposited; therefore, the most obvious mechanism of NRM acquisition would be detrital remanent magnetism (DRM), as indicated by the unstable demagnetization path and low NRM; however, the stability of the demagnetization path, shown in the lower breccia units (Fig. 3) and the high NRM, suggests that the temperature of these units, at the moment of deposition, was high enough to acquire their NRM by means of TRM rather than DRM.

As for the samples of the carbonate sequence, we suggest

that the mechanism of acquisition of their NRM is DRM. They show no obvious evidence of hydrothermal alteration and contain dark minerals and green glass shards supported in a dolomitic matrix. In the case of DRM, local effects associated with a high energy sedimentation regime could have prevented a stable record of the magnetic field. The presence of impact material in samples above the breccias, the higher concentration of such material in the lower samples (close to contact with the impact breccias), and the decrease of the same material toward the top of the sampled interval support the hypothesis that they were redeposited during the last stage modification phase of the formation crater (Melosh 1989). The dark minerals and glass shards are interpreted as reworked impact material and as the magnetic carrier in the carbonate sequence.

We note that DRM can yield shallower inclinations than the field inclination in which the sediment was deposited (e.g., Arason and Levi 1990; Levi and Banerjee 1990; Kent 1973). This phenomenon could be responsible for the rather shallow inclinations observed in samples Yax-1_794.14, Yax-1_794.59, and Yax-1_794.66.

The instability of some of the carbonate samples on top of the impact breccias might be associated with cross-bedding and interstratified horizons of coarser material (0.5 to 1.0 cm thick). These features suggest that this sequence was deposited in a sedimentary environment in which conditions were not stable at the moment of deposition (e.g., backwash, slumping); however, the absence of larger clasts (larger than a few cm) of impact material in the carbonate matrix and the low angle of the cross-bedding (<10°) suggests that the energy of the sedimentary environment was not very high; therefore, we must consider the possibility that the weak magnetic signal and, therefore, the instability of the demagnetization path could be the consequence of the absence of magnetic minerals in the interval.

Post-depositional remanent magnetism (PRM) is another possible recording mechanism for the NRM, and it comes from the observation that this interval is highly bioturbated by *Thalassinoides* and mottled with light and darker sediments. Keller (personal communication) found that *P. eugubina* are reworked into the burrows and suggested that Danian sediments mixed in with late Cretaceous sediments as a result of downward burrowing by *Thalassinoides* from the early Danian. The early Danian is also burrowed and mottled by *Thalassinoides* from above the K/T boundary to the top of the interval that was examined at 793.85 m. This suggests that the sediments above and below the K/T boundary have been perturbed, which could explain the erratic magnetic signals.

The location of Yax-1 was decided mainly on projections from the off-shore seismic lines (Bell et al. 2004); therefore, our most likely interpretation of the sedimentary process versus paleomagnetic signal relation is based on seismic reflection stratigraphy. Several authors had reported on the structure and post-impact sedimentary in-fill of the crater (Bell et al. 2004; Snyder and Hobbs 1999; Brittan et al. 1999; Morgan and Warner 1999; Christeson et al. 1999). According to these morphological and seismic stratigraphic models, Yax-1 was drilled on the flanks of the southern annular trough (Bell et al. 2004).

Bell et al. (2004) estimate that the deepest part of the annular trough contains the thickest section of the early Paleocene, and if the onshore annular trough has a similar sedimentary regime, there should be missing or thin sections of early Paleocene within Yax-1. This in agreement with the results presented here, with only 4–7 cm between the K/T boundary and the limit between chrons 29r to 29n.

Our plans are to continue with these detailed paleomagnetic analyses in the Yax-1 borehole core, upward and downward, and it is crucial to obtain other age constraints (either micropaleontology or radiometric, if possible) to be able to tie and correlate our geomagnetic polarity sequence.

Acknowledgments–This study forms part of the UNAM research program on the Chicxulub crater. Assistance with the laboratory analyses has been provided by Laboratoire des Sciences du Climat et l'Environnement, Gif-sur-Yvette, France. Partial financial support for this project has been provided by Conacyt grant G-25338-T. The authors thank Agnes Knotny (University of Heildelberg) for helpful discussions on the magnetic mineralogy. We also thank Gerta Keller (Princeton University) for providing helpful information and discussions on the sedimentology and micropaleontology of the K/T boundary. We are very grateful to Dick Norris (SCRIPPS) for helpful discussions and observations on a first draft of this article that helped us to improve it. We are also grateful to Jo Morgan (Imperial College) for comments on the article and to an anonymous reviewer. Rebolledo-Vieyra acknowledges Ph.D. grants from Conacyt, IMP, and UNAM, Conacyt grant G-25338-T, a post-doctoral grant from Conacyt, and support from CNRS, France for a post-doctoral position at LSCE.

Editorial Handling—Dr. Joanna Morgan

REFERENCES

Arason P. and S. Levi. 1990. Models of inclination shallowing during sediment compaction. *Journal of Geophysical Research* 95: 4481–4499.

Arz J. A., Alegret L., and Arenillas I. 2004. Foraminiferal biostratigraphy and paleoenvironmental reconstruction at Yaxcopoil-1 drill hole, Chicxulub crater, Yucatán Peninsula. *Meteoritics & Planetary Science* 39:1099–1111.

Bell C., Morgan J. V., Hampson G. J., and Trudgill B. 2004. Stratigraphic and sedimentary observations from seismic data across the Chicxulub impact basin. *Meteoritics & Planetary Science* 39:1089–1098.

Berggren W. A., Kent D. V., Swisher C. C., III, and Aubry M. P. 1995. A revised Cenozoic geochronology and chronostratigraphy. In *Geochronology, time scales, and global stratigraphic correlation,* edited by Berggren W. A. Special

Publication 54. Tulsa: Society for Sedimentary Geology. pp. 129–212.

Brittan J., Morgan J. V., Warner M., and Marin L. 1999. Near-surface seismic expression of the Chicxulub impact crater. In *Large meteorite impacts and planetary evolution II,* edited by Dressler B. O. and Sharpton V. L. Special Paper 339. Boulder: Geological Society of America. pp. 269–280.

Campos-Enríquez J. O., Arzate J. A., Urrutia-Fucugauchi J., and Delgado-Rodriguez O. 1997. The subsurface structure at the Chicxulub crater (Yucatán, Mexico): Preliminary results of a magnetotelluric study. *Leading Edge* 16:1774–1777.

Christeson G. L., Buffler R. T., and Nakamura Y. 1999. Upper crustal structure of the Chicxulub impact crater from wide-angle ocean bottom seismograph data. In *Large meteorite impacts and planetary evolution II,* edited by Dressler B. O. and Sharpton V. L. Special Paper 339. Boulder: Geological Society of America. pp. 291–298.

Dressler B. O., Sharpton V. L., Morgan J., Buffler R., Moran D., Smit J., Stöffler D., and Urrutia J. 2003. Investigating a 65-Ma-old smoking gun: Deep drilling of the Chicxulub impact structure. *Eos Transactions* 84:125.

French B. M. 1998. *Traces of a catastrophe: A handbook of shock-metamorphic effects in terrestrial meteorite impact structures.* Houston: Lunar and Planetary Institute.

Hildebrand A. R., Penfield G. T., Kring D. A., Pilkington M., Camargo A., Jacobsen S. B., and Boyton W. V. 1991. Chicxulub crater: A possible Cretaceous/Tertiary boundary impact crater on the Yucatán peninsula, Mexico. *Geology* 19: 867–871.

Keller G., Adatte T., Stinnesbeck W., Stüben D., Kramar U., and Harting M. 2003. The KT transition at Yaxcopoil-1 drillhole (abstract #10868). Geophysical Research Abstracts 5.

Keller G., Adatte T., Stinnesbeck W., Rebolledo-Vieyra M., Urrutia-Fucugauchi J., Kramar U., and Stüben D. 2004. Chicxulub impact predates the K-T boundary mass extinction. *Proceedings of the National Academy of Sciences* 101:3753–3758.

Kent D. V. 1973. Post-depositional remanent magnetization in deep-sea sediment. *Nature* 246:32–34.

Kirschvink J. L. 1980. The least-square line and plane and the analysis of palaeomagnetic data. *Geophysical Journal of the Royal Astronomical Society* 62:699–718.

Lerbekmo J. F., Sweet A. R., and Duke M. J. M. 1996. A normal polarity subchron that embraces the K/T boundary: A measure of sedimentary continuity across the boundary and synchroneity of boundary events. Special Paper 307. Boulder: Geological Society of America. pp. 465–476.

Levi S. and Banerjee S. 1990. On the origin of inclination shallowing in redeposited sediments. *Journal of Geophysical Research* 95: 4383–4389.

Melosh H. J. 1989. *Impact cratering: A geologic process.* New York: Oxford University Press.

Morgan J. V. and Warner M. 1999. Morphology of the Chicxulub impact: Peak-ring crater or multi-ring basin? In *Large meteorite impacts and planetary evolution II,* edited by Dressler B. O. and Sharpton V. L. Special Paper 339. Boulder: Geological Society of America. pp. 281–290.

Ortíz-Alemán C. 1999. Modelación Geofísica de Estructuras Complejas. Ph.D. thesis, Instituto de Geofisica, UNAM, México City, Mexico. 100 p.

Pilkington M. and Hildebrand A. 2000. Three-dimensional magnetic imaging of the Chicxulub crater. *Journal of Geophysical Research* 105:23479–23491.

Pope K. O., Ocampo A. C., Kinsland G. L., and Smith R. 1996. Surface expresion of the Chicxulub crater. *Geology* 24:527–530.

Rebolledo-Vieyra M, Urrutia-Fucugauchi J., Trejo-Garcia A., Marin L. E., Sharpton V. L., and Soler-Arechalde A. M. 2000. UNAM's scientific shallow drilling program into the Chicxulub impact crater. *International Geology Review* 42:948–972.

Sharpton V. L., Dalrymple G. B., Marin L. E., Ryder G., Shuraytz B. C., and Urrutia-Fucugauchi J. 1992. New links between the Chicxulub impact structure and the Cretaceous/Tertiary boundary. *Nature* 359:819–821.

Smit J., Buffler R., Moran D., Sharpton B., Stöffler D., Urrutia J., and Morgan J. 2003. Stratigraphy of the Yaxcopoil-1 drill hole in the Chicxulub impact crater (abstract #06498). Geophysical Research Abtracts 5.

Smit J., Van der Gaast S., and Lustenhouwer W. 2004. Is the transition impact to post-impact rock complete? Some remarks based on XRF scanning, electron-microprobe, and thin section analyses of the Yaxcopoil-1 core in the Chicxulub crater. *Meteoritics & Planetary Science* 39:1113–1126.

Snyder D. B. and Hobbs R. W. 1999. Deep seismic reflection profiles across the Chicxulub crater. In *Large meteorite impacts and planetary evolution II,* edited by Dressler B. O. and Sharpton V. L. Special Paper 339. Boulder: Geological Society of America. pp. 263–268.

Stinnesbeck W., Keller G., Adatte T., Harting M., Kramar U., and Stüben D. 2003. Yucatán subsurface stratigraphy based on the Yaxcopoil-1 drill hole (abstract #10868). Geophysical Research Abstracts 5.

Swisher C. C., Grajales-Nishimura J. M., Montanari A., Margolis S. V., Claeys P., Alvarez W., Renne P., Cedillo-Pardo E., Maurrasse F. J. R., Curtis G. H., Smit J., and McWilliams M. O. 1992. Coeval $^{40}Ar/^{39}Ar$ of 65.0 million years ago from Chicxulub Crater melt rock and Cretaceous-Tertiary boundary tektites. *Science* 257:954–958.

Urrutia-Fucugauchi J., Marin L., and Sharpton V. L. 1994. Reverse polarity magnetized melt rocks from the Cretaceous/Tertiary Chicxulub structure, Yucatán peninsula, Mexico. *Tectonophysics* 237:105–112.

Urrutia-Fucugauchi J., Marin L., and Trejo-Garcia A. 1996. UNAM Scientific drilling program of Chicxulub impact structure. Evidence for a 300 kilometer crater diameter. *Geophysical Research Letters* 23:1565–1568.

Urrutia-Fucugauchi J., Moran D. J., Sharpton V. L., Buffler R., Stoeffler D., and Smit J. 2001. The Chicxulub scientific drilling project (full proposal to International Continental Scientific Drilling Program). Mexico City: Institute of Geophysics, National University of Mexico. 45 p.

Ward W., Keller G., Stinnesbeck W., and Adatte T. 1995. Yucatán subsurface stratigraphy: Implications and constraints for the Chicxulub impact. *Geology* 23:873–876.